

A Compact Wideband Dual-Polarized Base Station Antenna Using Asymmetric Dipole

HAI LIN¹ (Member, IEEE), WEN YU¹ (Graduate Student Member, IEEE), FANGSHUN DENG²,
BAIHUI LIAO³, AND RONGXIN TANG⁴ (Member, IEEE)

¹College of Physical Science and Technology, Central China Normal University, Wuhan 430079, China

²Laboratory of Low-Frequency Electro-Magnetic Communication Technology, 722 Research Institute, CSIC, Wuhan 430079, China

³Research and Design Department, Shenzhen Xinlong Communication Technology Company, Ltd., Shenzhen 518116, China

⁴Institute of Space Science and Technology, Nanchang University, Nanchang 330021, China

CORRESPONDING AUTHORS: H. LIN AND R. TANG (e-mail: linhai@mail.ccnu.edu.cn; rongxint@ncu.edu.cn)

This work was supported in part by the Fundamental Research Funds for the Central University of China under Grant CCNU20GF004 and Grant CCNU19TS073; in part by the open fund of Guangxi Key Laboratory of Wireless Wideband Communication and Signal Processing under Grant GXKL06190202; in part by the open fund of China Ship Development and Design Centre under Grant XM0120190196; in part by the National Natural Science Foundation of China under Grant 41974195; and in part by the Hongque Innovation Center under Grant HQ202104001.

ABSTRACT A compact wideband dual-polarized antenna for base station application is proposed. The antenna element consists of a main radiator, two baluns, and a reflector. Two methods are used to enhance bandwidth and improve the port-to-port isolation. Firstly, by integrating the parasitic elements to traditional dipoles, new resonant modes are introduced to realize broadband, which can be controlled flexibly. Subsequently, part of the parasitic elements is removed to form asymmetric dipoles. Due to the asymmetry construction of the design, the polarization isolation of the antenna achieves more than 30 dB in the whole working band with stable radiation patterns. In addition, the specially designed parasitic elements achieve enhanced bandwidth without increasing the size of the radiator. The Simulation and measurement results show that the antenna has an impedance bandwidth of 32.7% (690-960 MHz). Moreover, a stable half-power beamwidth (HPBW) of $68^\circ \pm 5^\circ$ and a high gain of 8.5 ± 0.3 dBi is achieved. To verify the performance of the antenna, a compact high-gain base station array was designed and manufactured. The good performance of the proposed antenna makes it a promising candidate for 4G/5G base station application.

INDEX TERMS Base station antenna, broadband, dual-polarized, asymmetric dipole.

I. INTRODUCTION

WITH the development of wireless communication technology, the operation bands of the base station system have been widely extended, more antenna subarrays with enhanced bandwidth need to be deployed for different applications [1]–[5]. Since the volume of the base station system is limited, newly deployed antennas must have a compact size [6]–[9]. On the other hand, the mutual coupling has been a serious issue due to the compact spacing between different antenna subarrays [10]–[13]. Designing the base station antenna which can solve the above problems has become a research hotspot.

At present, a large number of broadband antennas have been proposed for base station applications [14]–[19]. The most common manner to increase its bandwidth is to integrate parasitic elements. In [14], parasitic cross dipoles are embedded into the gap of the crossed loop dipoles, thus a broadband dual-polarized antenna achieved a relative bandwidth of 54.5% (1.68-2.94 GHz). In [17], 4 layers of circular parasitic patches were added to the top of the U-shaped slot dipoles, a relative bandwidth of 67% (1.39-2.8 GHz) is obtained. Since the parasitic elements are mostly loaded around or above the radiator, this will not only increase the size of the antenna but also introduce new scattering sources

to the antenna system and cause stronger mutual coupling. Another method is to create the magneto-electric (ME) resonance in the dipole radiator. The ME dipole designed in [18] has a stable radiation pattern covering the 1.7-2.7 GHz frequency band but its design process is quite complicated.

For base station application, it is also critical to effectively reduce the volume of the antenna which normally relies on the special structure design of the radiators [20]–[22]. For example, in [20], multiple resonance points are generated through the connecting line to meet the design requirements on size and bandwidth. In [21], it proposed a compact broadband antenna by introducing spline-edged bowties as the radiator, which widened the current path to achieve enhanced bandwidth and shrunk size. However, these antennas often require complicated designs and cannot flexibly control their resonance modes.

In this paper, a compact wideband base station antenna is proposed, which aims to achieve broad impedance bandwidth in LB with low complexity as well as improved port-to-port isolation. The cross dipoles are chosen as the initial design because this structure can easily achieve $\pm 45^\circ$ polarization, and the radiation arm of the antenna is small, which can effectively reduce the shielding of the HB elements in the array. However, the antenna is limited by its bandwidth and can not cover LB. Therefore, the parasitic elements were introduced to the cross dipoles to flexibly control two resonant modes. Subsequently, we remove part of the parasitic elements to form asymmetric dipoles, which significantly improve the polarization isolation without beam squint. In addition, the specially designed parasitic elements only expand the bandwidth of the antenna and do not introduce new scattering sources and affect the radiation patterns. Moreover, due to the proposed antenna is made of aluminum, in the simulation, its radiation efficiency is close to 100%. Simulation and measurement results show that the antenna achieves an impedance bandwidth of 32.7% (690-960 MHz). Moreover, a stable half-power beamwidth (HPBW) of $68^\circ \pm 5^\circ$ and a high gain of 8.5 ± 0.3 dBi is obtained. A compact high-gain base station array was fabricated to verify the radiation performance and design freedom of the proposed antenna.

II. ANTENNA CONFIGURATION

The Configuration of the proposed antenna is shown in Fig. 1. It can be seen that the antenna is composed of a radiator, two baluns, a bedframe, and a reflector. All the structures are made of aluminum. Fig. 2 shows the special design of the radiator. As depicted, the radiator consists of two pairs of bent asymmetric dipoles. Different from the traditional half-wavelength dipole, only one arm of the asymmetric dipole are integrating with a pair of parasitic elements. This special structure can not only realize good radiation performance with enhanced bandwidth but also achieve more than 30 dB polarization isolation compared to normal dipoles. In addition, the shrunk size of the radiating arm provides more design freedom in array fabrication. The detail of the baluns

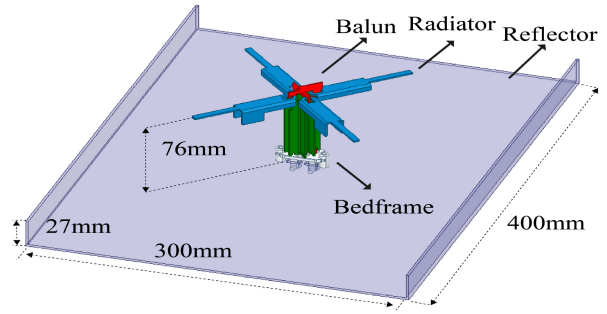


FIGURE 1. Configuration of the proposed antenna.

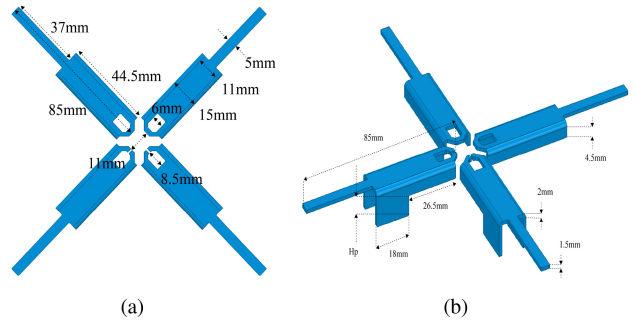


FIGURE 2. Detail of (a) top view and (b) side view of the radiator, $H_p = 8.5$ mm.

is shown in Fig. 3. The two pairs of baluns are fed by two 50Ω coaxial cables at the bottom. The baluns are made of aluminum, which can reduce feeding loss, ensuring high radiation performance. Fig. 4 shows the details of the bedframe, which is used to fasten the baluns to the reflector. After parameter optimization, a compact antenna with excellent radiation performance is proposed.

III. PARAMETRIC STUDY

In this section, an antenna composed of traditional dipoles that has a single resonating mode leads to a narrow impedance bandwidth is designed, firstly. Then, four pairs of rectangular parasitic elements are integrating to the dipoles, thus, a new resonating mode is introduced and the two resonating modes can be flexibly controlled by tuning the length and width of the parasitic elements to realize enhanced bandwidth. Moreover, two pairs of parasitic elements are removed to achieve better polarization isolation. Finally, a three-dimensional asymmetric cross dipole with miniaturization aperture is proposed.

Firstly, a dual-polarized base station antenna that works in the desired band is designed. As shown in Fig. 5(a), two pairs of simple cross dipoles form the radiator, the length of the dipoles is 181 mm, which is half-wavelength of the center frequency of the base station’s low-frequency band. According to the simulated S-parameters with different L values shown in Fig. 5(b), the initial design has only one resonating mode in the working band. Its resonance frequency changes with the values of L accordingly. Due to the simple structure design, the impedance bandwidth of the initial

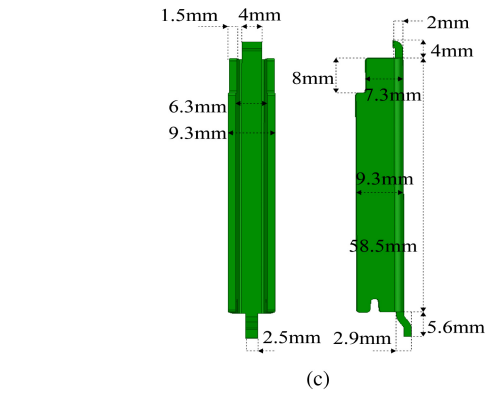
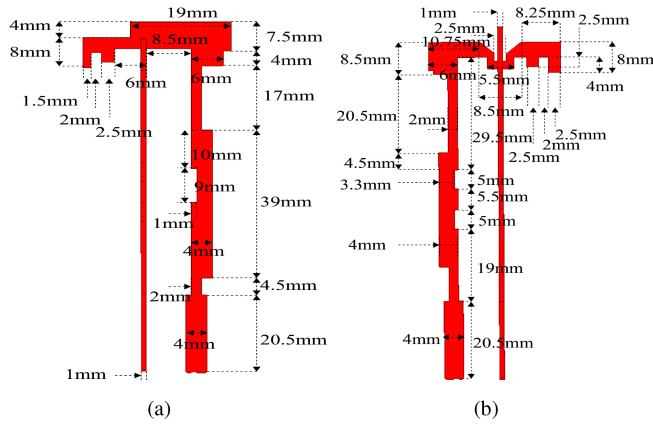


FIGURE 3. Detail of the feeding structures.

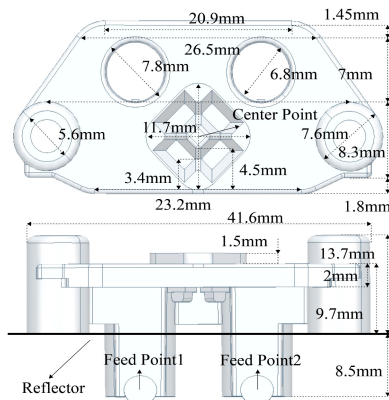


FIGURE 4. Detail of the bedframe.

design is limited. In addition, the polarization isolation of the antenna is quite poor, therefore, several effective methods must be taken to improve the overall performance of the initial design.

To enhance the bandwidth of the antenna, a new resonating mode must be introduced. Therefore, an improved design which two pairs of rectangular parasitic elements are added to each dipole is shown in Fig. 6(a). The simulated S-parameters with different parameters of L_p and W_p are shown in Figs. 6(d) and (e), respectively. As depicted, through changing the length of the rectangular parasitic

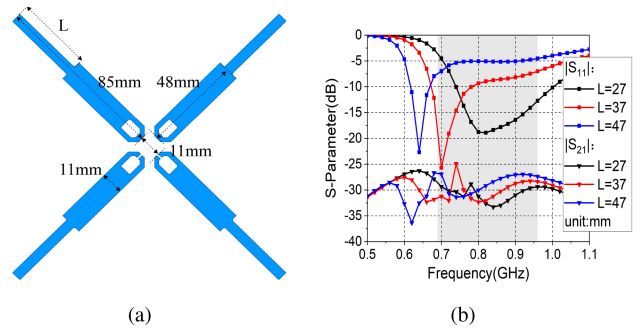


FIGURE 5. (a) The detail of the initial cross dipoles. (b) The simulated S-parameters with different L of the dipoles.

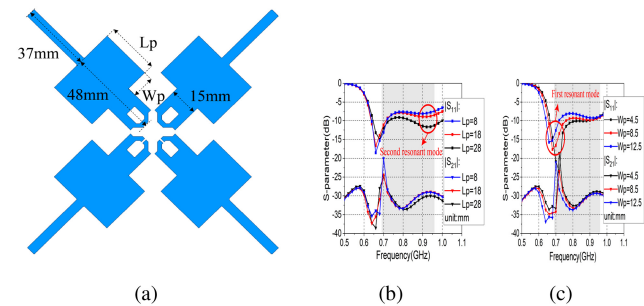


FIGURE 6. (a) The detail of the improved cross dipoles. (b) The current distribution of the first resonance mode. (c) The current distribution of the second resonance mode. (d) The simulated S-parameters with different L_p of the dipoles, $W_p = 12.5$ mm. (e) The simulated S-parameters with different W_p of the dipoles, $L_p = 18$ mm.

element, the second resonance mode was introduced and the impedance bandwidth of the antenna might be improved. On the other hand, the frequency of the first resonance mode moves to the second one with the decrease of W_p . Therefore, optimize the length and width of the rectangular parasitic elements at the same time can bring the two resonating modes closer to achieve desired bandwidth. To prove the concept, the surface current distribution of two modes are shown in Figs. 6(b) and (c). However, no matter how to optimize the parameter combinations, the polarization isolation around the first resonating frequency of the design will always be degraded, this can be considered to be the introduction of parasitic elements that strengthened the resonance of this mode, resulting in the strong coupling. Therefore, special methods need to be adopted to design the parasitic elements efficiently without modifying the antenna's radiation performance.

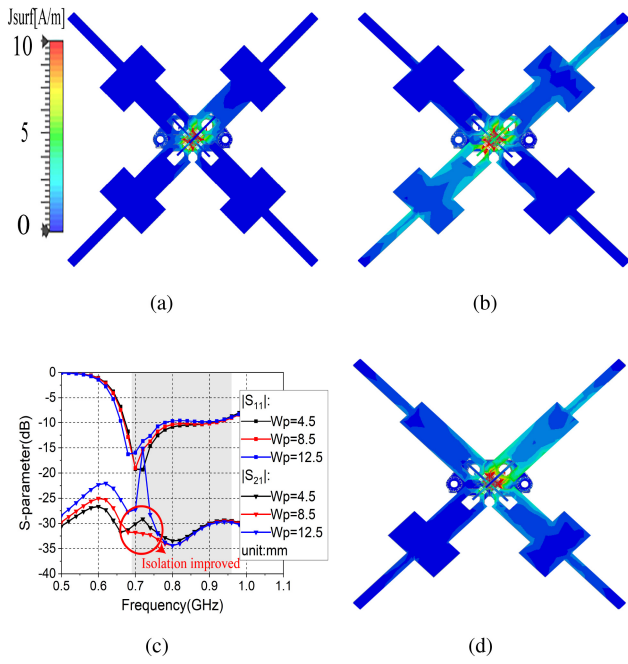


FIGURE 7. (a) Surface current distribution of the improved dipole at 720 MHz. (b) Surface current distribution of the improved dipole at 800 MHz. (c) The simulated S-parameters with different W_p of the asymmetric dipoles, $L_p = 18$ mm. (d) Surface current distribution of the asymmetric dipole at 720 MHz.

To improve the polarization isolation, we first studied the surface current distribution of the improved dipole at 720 MHz and 800 MHz which are shown in Figs. 7(a) and (b), respectively. The isolation deterioration occurs at 720 MHz, which is the resonance frequency of the half-wave dipole, the current distributed at the radiation arms is weakened, the unwanted current is coupled from the feeding port to another port, resulting in deterioration of isolation. At 800 MHz, the surface current mainly distributes at the radiation arms, which realizes good polarization isolation. Therefore, to solve the polarization isolation degradation problem, a pair of rectangular parasitic elements are removed from each dipole to shift the current at the resonance frequency. The simulated S-parameters with different W_p of the rectangular parasitic element are shown in Fig. 7(c). It is obvious that varying the width of the rectangular parasitic elements can still improve the impedance matching of the first resonance mode. When the width of the rectangular parasitic elements is $W_p = 8.5$ mm, the polarization isolation of the antenna in the operating band exceeds 30 dB. The surface current distribution of the modified dipole at 720 MHz is shown in Fig. 7(d). It can be noticed that after removing rectangular parasitic elements, the surface current mainly concentrated on the radiating arms at the resonance frequency. In other words, the current coupling to the other port has been reduced, thus the polarization isolation in the working band has been increased to more than 30 dB.

Although the asymmetric dipole enhances the polarization isolation of the antenna, this asymmetry may damage the radiation performance. For this reason, analysis of HPBW

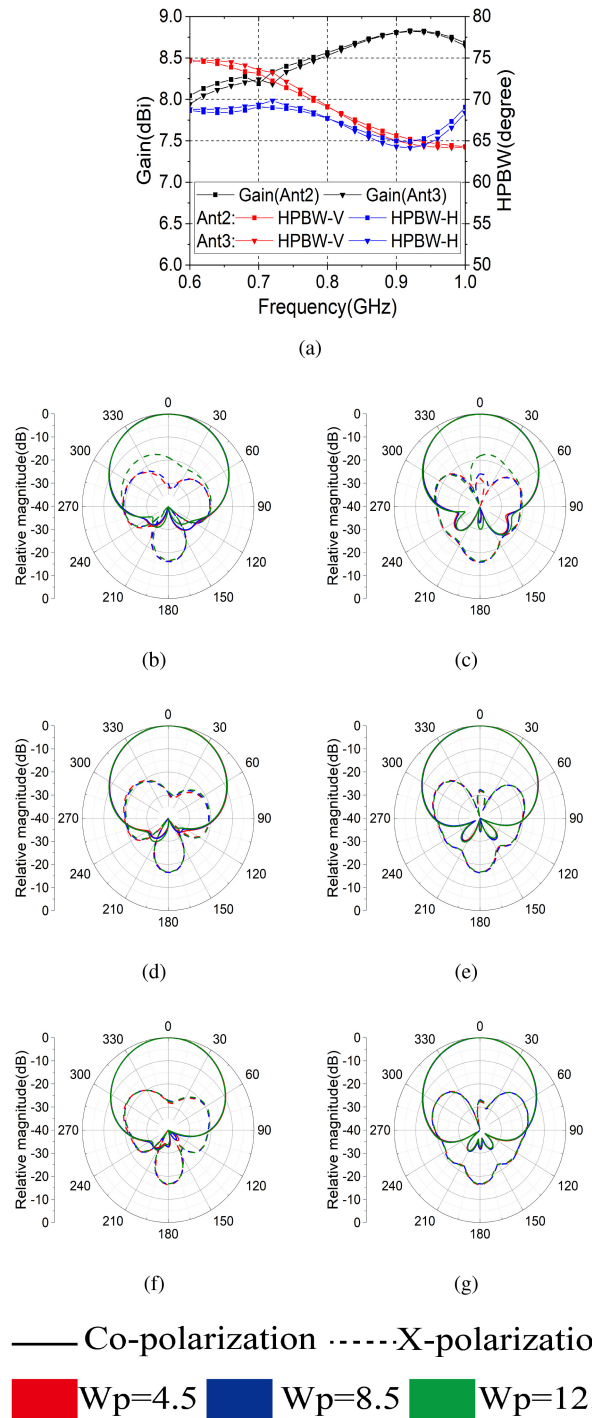


FIGURE 8. (a) Simulated Gain and HPBWs of the improved dipole (Ant2) and asymmetric dipole (Ant3), $W_p = 8.5$ mm, $L_p = 18$ mm. Normalized $+45^\circ$ -plane radiation patterns of Ant3 with different values of W_p at (b) 700 MHz, (d) 800MHz, and (f) 900 MHz. Normalized -45° -plane radiation patterns of Ant3 with different values of W_p at (c) 700 MHz, (e) 800MHz, and (g) 900 MHz.

and gain should be taken, and the results are shown in Fig. 8(a), where Ant2 refers to the improved traditional dipole and Ant3 refers to the asymmetric dipole. As can be seen, after removing a pair of parasitic elements from the arm of the dipole, the gain has dropped slightly, but HPBW

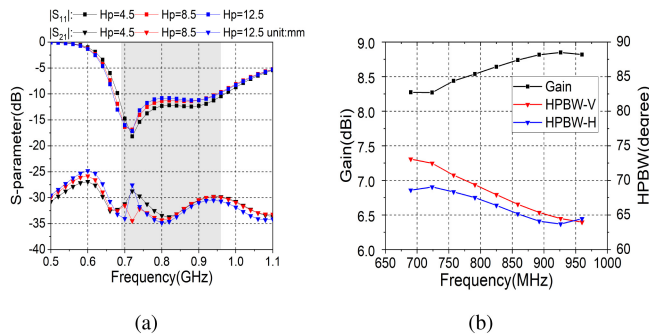


FIGURE 9. (a) The simulated S-parameters with different H_p of the proposed antenna. (b) The simulated Gain and HPBWs of the proposed antenna.

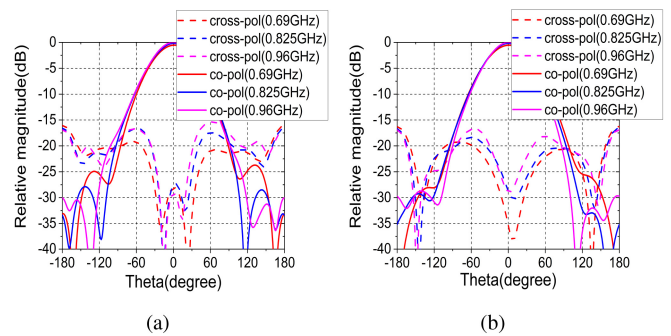


FIGURE 10. (a) The simulated radiation patterns for H-Plane. (b) The measured radiation patterns for V-Plane.

is very stable, almost the same as before. To further study the role of parasitic elements, we compare their radiation patterns at different frequencies by varying W_p , the results are shown in Figs. 8(b)–(g). As depicted, varying the width of parasitic elements has almost no effect on the radiation performance of the antenna. It can be proved that the asymmetric dipole can maintain good radiation performance while improving polarization isolation. This can also be proved by studying the current distribution in Fig. 6. The current is mainly distributed at the center of the dipole. Therefore, the asymmetric dipole introduces a new resonance mode to expand the bandwidth and avoids the deterioration of isolation caused by the introduction of parasitic elements.

Since parasitic elements added to the LB antennas will block the HB antennas in a LB-HB array, we tried to bend and extend the parasitic elements downward to reduce the obstruction in the final design as shown in Fig. 2. The simulated S-parameters with different H_p of the final design is shown in Fig. 9(a), and the simulated gain and HPBWs of the proposed antenna is shown in Fig. 9(b). As depicted, for $H_p = 8.5$ mm, the antenna has achieved an enhanced bandwidth of 690-960 MHz ($|S_{11}| < -10$ dB) and more than 30 dB in-band polarization isolation. Moreover, the stable HPBWs of $68 \pm 5^\circ$, the gain of 8.5 ± 0.3 dBi are obtained over the operating band.

IV. RESULT AND DISCUSSION

The proposed antenna is manufactured and measured to verify the simulation result. Fig. 10 shows the simulated radiation patterns of the proposed antenna while port-1 is excited. As depicted, within the $-60^\circ \leq \theta \leq +60^\circ$ region, a XPD (cross-polar discrimination) > 5 dB is obtained, and the cross-polarization within the main lobe is smaller than 26 dB at the broadside direction ($\theta = 0^\circ$).

For application, a compact high-gain base station array is fabricated, which composes of the proposed antennas and HB elements whose radiation performance are similar to the HB elements reported in [23], detail of the array is shown in Fig. 11(a), the photograph of the array is shown in Fig. 11(b). The array composes of a column of 11-unit LB elements and two columns of 12-unit HB elements. The LB elements spacing 250 mm, approximately $0.69 \lambda_0$, and the

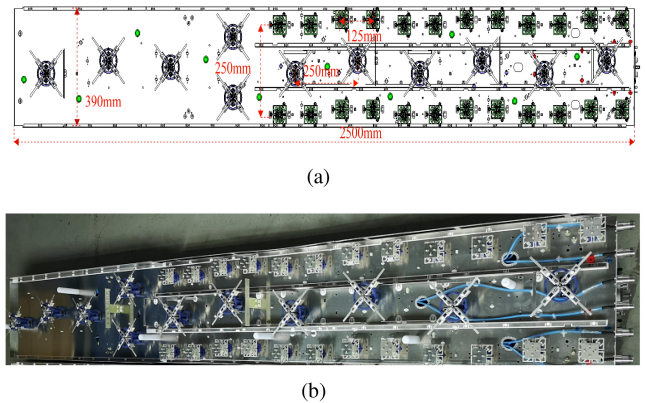


FIGURE 11. (a) The layout of the base station array. (b) The photograph of the base station array.

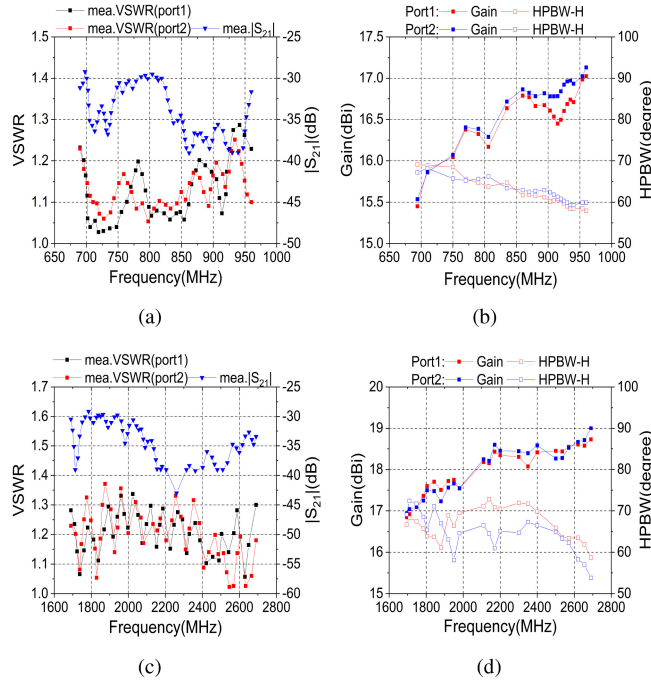
HB elements spacing 125 mm, approximately $0.92 \lambda_0$. The width of the array is 390 mm, which has a very compact width for the base station application.

The measured result of the array is shown in Fig. 12. As depicted in Figs. 12(a) and (b), the measured S-parameters of the proposed antenna show broad impedance bandwidth of 32.7% (690-960 MHz) for $VSWR < 1.3$ and polarization isolation of more than 29 dB in the operating band. Besides, the 11-unit LB elements achieve a stable HPBWs of $63 \pm 5^\circ$ and a high gain of 16.4 ± 0.9 dBi. On the other hand, the HB elements also realize a good radiation performance. As depicted in Figs. 12(c) and (d), a broad impedance bandwidth of 44.5% (1710-2690 MHz) for $VSWR < 1.4$ and polarization isolation of more than 29 dB in HB are obtained. Moreover, the radiation performance of a column of 12-unit HB elements is also measured, it has stable HPBWs of $63 \pm 9^\circ$ along with high gain of 18 ± 1 dBi. Therefore, a compact high-gain base station array with good performance is fabricated and measured.

To further illustrate the advantages of the proposed antenna, the comparison between the proposed antenna and the other antennas in terms of size, bandwidth, gain, HPBW, and polarization isolation is shown in Table 1. The comparison results show that the proposed antenna element has smaller radiating arm size which achieves smaller aperture. In [5], parasitic elements are loaded around the radiator to enhance bandwidth, but this method will increase the size

TABLE 1. The comparison of various parameters between the proposed antenna and other antennas.

Ref.	Size(λ_0^3 , without reflector)	Broadband technique	Bandwidth(Gain, VSWR<1.5)	Gain(dBi)	HPBW(H-plane)	Isolation(dB)
[4]	$0.44\lambda_0 \times 0.44\lambda_0 \times 0.24\lambda_0$	Slot	1.68-2.74(48%)	8.2	$62.5^\circ \pm 3.5^\circ$	>22
[5]	$0.51\lambda_0 \times 0.51\lambda_0 \times 0.26\lambda_0$	Parasitic element	1.7-2.9(52%)	8.5	$65^\circ \pm 5^\circ$	>25
[17]	$0.46\lambda_0 \times 0.46\lambda_0 \times 0.35\lambda_0$	Parasitic element	1.39-2.8(67%)	9	$68^\circ \pm 4^\circ$	>30
[21]	$0.54\lambda_0 \times 0.54\lambda_0 \times 0.24\lambda_0$	None	1.42-2.9(68%)	8	$65^\circ \pm 11^\circ$	>20
This work	$0.5\lambda_0 \times 0.5\lambda_0 \times 0.21\lambda_0$	Parasitic element	0.69-0.96(32.7%)	8.5 ± 0.3	$68^\circ \pm 5^\circ$	>30


FIGURE 12. (a) The measured S-parameters of the array in LB. (b) The measured Gain and HPBWs of the array in LB. (c) The measured S-parameters of the array in HB. (d) The measured Gain and HPBWs of the array in HB.

of the radiator, and this work does not further improve the port-to-port isolation. Moreover, the form of differentially fed will increase the required feed ports. In [17], the bandwidth is enhanced by stacking four layers of parasitic elements, and the isolation also meets the application requirements. However, it should be noted that this method will greatly increase the height of the antenna which does not meet the needs of reducing the volume of the antenna. Compare with the above results, the proposed antenna only uses parasitic elements to realize enhanced bandwidth without increasing the size of the radiator and maintain good radiation performance, demonstrated how to use parasitic elements to complete a low-complexity broadband LB antenna. Finally, although the size of the antenna does not show significant advantages, its cross structure can minimize the shielding for high-frequency elements in the base station array, thereby providing more freedom in array design.

V. CONCLUSION

In this paper, a compact wideband dual-polarized base station antenna using asymmetric dipole is proposed. With the integration of parasitic elements, two resonating modes are realized to achieve broad impedance bandwidth. Compared with symmetrical dipoles, asymmetrical dipoles achieve

higher polarization isolation. Besides, a low complexity structure is proposed to achieve more design freedom in base station array. The measured result shows that a broad impedance bandwidth of 32.7% (690-960 MHz) for VSWR<1.5, high polarization isolation of more than 29 dB, stable HPBW of $68^\circ \pm 5^\circ$ and high gain of 8.5 ± 0.3 dBi are obtained in whole LB. In addition, a compact high-gain base station array is fabricated to verify the performance of the proposed antenna, a broad impedance bandwidth of 44.5% (1710-2690 MHz) for VSWR<1.4 and polarization isolation of more than 29 dB in HB are obtained. good measurement results indicate that the designed antenna has achieved the expected performance. Thus, it is a good candidate for the LB element of side-by-side multi-band multi-array base station antennas.

ACKNOWLEDGMENT

The authors would like to thank Shenzhen Xinlong Communication Technology Company for array fabrication and measurement.

REFERENCES

- [1] H. Sun, C. Ding, B. Jones, and Y. J. Guo, "A wideband base station antenna element with stable radiation pattern and reduced beam squint," *IEEE Access*, vol. 5, pp. 23022–23031, 2017.
- [2] A. Alieldin, Y. Huang, S. J. Boyes, M. Stanley, S. D. Joseph, and B. Al-Juboori, "A dual-broadband dual-polarized Fylfot-shaped antenna for mobile base stations using MIMO over-lapped antenna subarrays," *IEEE Access*, vol. 6, pp. 50260–50271, 2018.
- [3] Y. He, W. Tian, and L. Zhang, "A novel dual-broadband dual-polarized electrical downtilt base station antenna for 2G/3G applications," *IEEE Access*, vol. 5, pp. 15241–15249, 2017.
- [4] H. Huang, Y. Liu, and S. Gong, "A broadband dual-polarized base station antenna with sturdy construction," *IEEE Antennas Wireless Propag. Lett.*, vol. 16, pp. 665–668, 2016.
- [5] D.-L. Wen, D.-Z. Zheng, and Q.-X. Chu, "A wideband differentially fed dual-polarized antenna with stable radiation pattern for base stations," *IEEE Trans. Antennas Propag.*, vol. 65, no. 5, pp. 2248–2255, May 2017.
- [6] L.-H. Wen, S. Gao, Q. Luo, Q. Yang, W. Hu, and Y. Yin, "A low-cost differentially driven dual-polarized patch antenna by using open-loop resonators," *IEEE Trans. Antennas Propag.*, vol. 67, no. 4, pp. 2745–2750, Apr. 2019.
- [7] C. Ding, H. Sun, R. W. Ziolkowski, and Y. J. Guo, "Simplified tightly-coupled cross-dipole arrangement for base station applications," *IEEE Access*, vol. 5, pp. 27491–27503, 2017.
- [8] H. Zhai, L. Xi, Y. Zang, and L. Li, "A low-profile dual-polarized high-isolation MIMO antenna arrays for wideband base-station applications," *IEEE Trans. Antennas Propag.*, vol. 66, no. 1, pp. 191–202, Jan. 2018.
- [9] L. Y. Nie *et al.*, "A low-profile coplanar dual-polarized and dual-band base station antenna array," *IEEE Trans. Antennas Propag.*, vol. 66, no. 12, pp. 6921–6929, Dec. 2018.
- [10] B. Feng, K. L. Chung, J. Lai, and Q. Zeng, "A conformal magneto-electric dipole antenna with wide H-plane and band-notch radiation characteristics for sub-6-GHz 5G base-station," *IEEE Access*, vol. 7, pp. 17469–17479, 2019.

- [11] Y. Liu, S. Wang, N. Li, J.-B. Wang, and J. Zhao, "A compact dual-band dual-polarized antenna with filtering structures for sub-6 GHz base station applications," *IEEE Antennas Wireless Propag. Lett.*, vol. 17, pp. 1764–1768, 2018.
- [12] Y. Li, Z. Zhao, Z. Tang, and Y. Yin, "Differentially fed, dual-band dual-polarized filtering antenna with high selectivity for 5G sub-6GHz base station applications," *IEEE Trans. Antennas Propag.*, vol. 68, no. 4, pp. 3231–3236, Apr. 2020.
- [13] Q.-X. Chu, Y.-L. Chang, and J.-P. Li, "Crisscross-shaped $\pm 45^\circ$ dual-polarized antenna with enhanced bandwidth for base stations," *IEEE Trans. Antennas Propag.*, vol. 69, no. 4, pp. 2341–2346, Apr. 2021.
- [14] D.-Z. Zheng and Q.-X. Chu, "A wideband dual-polarized antenna with two independently controllable resonant modes and its array for base-station applications," *IEEE Antennas Wireless Propag. Lett.*, vol. 16, pp. 2014–2017, 2017.
- [15] J. Wang, L. Zhao, Z.-C. Hao, and J.-M. Jin, "A wideband dual-polarized omnidirectional antenna for base station/WLAN," *IEEE Trans. Antennas Propag.*, vol. 66, no. 1, pp. 81–87, Jan. 2018.
- [16] Z. Tang, J. Liu, Y.-M. Cai, J. Wang, and Y. Yin, "A wideband differentially fed dual-polarized stacked patch antenna with tuned slot excitations," *IEEE Trans. Antennas Propag.*, vol. 66, no. 4, pp. 2055–2060, Apr. 2018.
- [17] Y. Cui, L. Wu, and R. Li, "Bandwidth enhancement of a broadband dual-polarized antenna for 2G/3G/4G and IMT base stations," *IEEE Trans. Antennas Propag.*, vol. 66, no. 12, pp. 7368–7373, Dec. 2018.
- [18] C. Ding, H.-H. Sun, R. W. Ziolkowski, and Y. J. Guo, "A dual layered loop array antenna for base stations with enhanced cross-polarization discrimination," *IEEE Trans. Antennas Propag.*, vol. 66, no. 12, pp. 6975–6985, Dec. 2018.
- [19] R. Wu and Q.-X. Chu, "A wideband dual-polarized antenna for LTE700/GSM850/GSM900 applications," *IEEE Antennas Wireless Propag. Lett.*, vol. 16, pp. 2098–2101, 2017.
- [20] H.-H. Sun, C. Ding, H. Zhu, and Y. J. Guo, "Dual-polarized multi-resonance antennas with broad bandwidths and compact sizes for base station applications," *IEEE Open J. Antennas Propag.*, vol. 1, pp. 11–19, 2019.
- [21] Q. Zhang and Y. Gao, "A compact broadband dual-polarized antenna array for base stations," *IEEE Antennas Wireless Propag. Lett.*, vol. 17, pp. 1073–1076, 2018.
- [22] D. Zheng, Y. Luo, and Q.-X. Chu, "A miniaturized wideband dual-polarized antenna based on mode-control principle for base-station applications," *IEEE Access*, vol. 8, pp. 62218–62227, 2020.
- [23] W. Chen *et al.*, "A low profile broadband dual-polarized base station antenna using folded dipole radiation element," *IEEE Access*, vol. 7, pp. 67679–67685, 2019.